

# A True Random Number Generator Method Embedded in Wireless Communication Systems

Toshinori Suzuki, and Masahiro Kaminaga\*

November 28, 2018

## Abstract

To increase the number of wireless devices, e.g., mobile or IoT terminals, cryptosystems are essential for secure communications. In this regard, random number generation is crucial because the appropriate function of cryptosystems relies on it to work properly. This paper proposes a true random number generator (TRNG) method capable of working in wireless communication systems. By embedding a TRNG in such systems, no additional analog circuits are required and working conditions can be limited as long as wireless communication systems are functioning properly, making TRNG method cost-effective. We also present some theoretical background and considerations. We next conduct experimental verification, which strongly supports the viability of the proposed method.

## 1 Introduction

Random number generation is a crucial aspect for many forms of secure communications, since it is indispensable in cryptosystems, which have their security based on the assumption that the numbers are truly random. Some shortcomings have been found in the practical application of these types of security systems due to insufficient randomness. The digital signature algorithm (DSA) is an example requiring random numbers for every signature. For this algorithm the secret key can be recovered after a few signatures when using a pseudo-random number (PRN) generator [1]. Even DSA private keys of SSH hosts can be obtained to some extent because of insufficient signature randomness [2]. Considering these circumstances, statistical randomness alone is not enough and unpredictability is necessary. Compared with a PRN generated deterministically from a seed number, a true random number (TRN) is nondeterministic; therefore, from the viewpoint of security, a TRN is preferable. Accordingly, the source of the TRN is an important practical issue based on both cost and performance.

---

\*T. Suzuki and M. Kaminaga are with the Department of Information Technology Engineering, Tohoku Gakuin University, 13-1, Chuo-1, Tagajo, 985-8537, Japan e-mail: (tn.suzuki@mail.tohoku-gakuin.ac.jp).

True random number generator (TRNG) methods that use a noise source are mainly classified into three categories [3], including (1) direct amplification, (2) oscillator sampling, and (3) discrete-time chaos. Method (1) amplifies unpredictable noise and compares it with an appropriate threshold to determine whether to assign it with a 0 or 1 at the time of sampling [4]. Due to the necessity of wide-band amplification by analog circuits, method (1) requires additional analog circuits. These circuits are rather expensive. Method (2) latches jittery output from a fast oscillator with a slow clock, whereas method (3) magnifies the uncertainty of noise using nonlinear analog mapping and positive feedback. Compared with methods (1) and (3), method (2) has merit based on the cost because it can be integrated with signal processing circuits and performs well against  $1/f$  noise and amplifier offset [5].

For small IoT terminals, e.g., wireless sensors and RFIDs, TRNGs should have less impact on hardware and power consumption because of poor resource in such terminals. Efforts to minimize impacts associated with hardware have been found to have succeeded in improving circuit implementation in accordance with methods (1) and/or (2). A previous study [6] shows a TRNG from thermal noise by  $3 \mu\text{W}$  power consumption, even after cancelling unpreferable components, e.g., DC offset or slowly varying noise. The method used therein is based on method (1) although a latch is used instead of a direct amplifier to sample the noise. These latch-based TRNGs are a variation of method (1). Similar TRNG methods based on thermal noise are found in previous research [7] wherein feedback circuit has been used instead of operational amplifier and comparator. Aiming at RFIDs, which require less power consumption and less hardware complexity, Balachandran *et al.* [8] exploited a jittery 320 kHz internal clock to sample the RF signal used for 900 MHz RFID systems. As an additional circuit, noise buffer was introduced to give the jitter to the internal clock. With other supplemented components, the circuit consumes only 440 nA. This method generates a 3-bit TRN at a time to prevent RFID collision. In previous research [5], not only anticollision with a few bits of the TRN, but secure communication is also realized at a cost of  $1.04 \mu\text{W}$  using a postdigital processor.

Another approach makes use of some hardware that are originally equipped in target terminals. A previous study [9] employed a visible spectrum measured by an image sensor as a random source, another research [10] employed accelerometers for an RNG. Other sensors and input devices, e.g., microphone, magnetometer, gyroscope, keyboard, mouse devices, are also candidates that capture a randomness [11]. This approach requires measurements and processing, and it may consume more battery and time. However, it may not require additional circuits depending on the terminal. An important component of the wireless terminal is the radio frequency (RF) module because it is necessary for the device to serve its intended purpose. TinyRNG [12] exploits bit errors in wireless links as a random source. Latif *et al.* [13] used the fluctuation of a received signal strength indicator, the shortcomings of which were later identified by Hennebert *et al.* [14] and improved it by incorporating a link quality indicator. However, these methods still require additional measurements and processing, which consumes battery and time for a TRNG.

The RF module is typically composed of a signal amplifier, local oscillator and an analog-to-digital converter (ADC) for digital demodulation. Although the amplifier is referred to as a low-noise amplifier since the high gain is sufficient for amplifying weak radio waves, noise is usually contained in the signal after the ADC. With respect to wireless link, signal detection is realized by combating against noises. In other words, wireless devices contain a considerable amount of noise.

This paper proposes to exploit the noise contained in the received signal after the ADC to enhance TRNG performance. Unlike conventional methods [12]-[14] which require additional signal measurements and processing, our method exploits discarded data at physical layers in wireless communication links. It is therefore likely to be efficient and has a higher TRNG throughput according to the sampling rate of the physical layer. Experimental evaluations show that the proposed scheme performs well compared with conventional schemes for wireless mobile terminals.

The remainder of this paper is organized as follows. Section 2 presents a feature and a model of thermal noise for the conventional TRNG method (1), which becomes a contrast to our proposed TRNG scheme. Section 3 presents the theoretical background and the concept of the proposed TRNG method, which is depicted with system configuration and theoretical evaluation in Section 4. In Section 5, the feasibility of the proposed method is experimentally verified with a software defined radio (SDR) device. Section 6 concludes this paper.

## 2 Conventional TRNG uses MSB of noise source

For conventional TRNG methods using thermal noise, the noise level determines the random number. Therefore, in such methods, unpredictable components should be dominant in the noise. However, in general, the noise usually brings unpreferable components such as  $1/f$  noise, AC line noise, and so on. In a previous study [3], the noise model shown in Fig. 1 was used to compare the randomness of TRNG methods (1)-(3) when the source comprised unpreferable components. In Fig. 1, PRNG refers to a Gaussian pseudo-RNG, and  $n_A(t)$

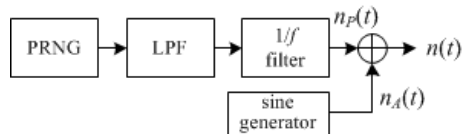


Figure 1: Noise model for TRNG method evaluation in [3].

means coupling sinusoidal noise.  $n_P(t)$  follows Gaussian distribution, and its power spectrum takes the general form presented in Fig. 2.

The corner frequency  $f_{co}$  depends on the implementation technology. It has been reported that the  $f_{co}$  is on the order of a few tens of hertz for JFETs and a few tens to hundreds of kilohertz for MOSFETs [15]. In particular, for

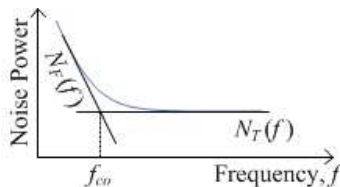


Figure 2: Typical noise power spectrum of  $n_P(t)$ .

MOSFETs with a width of a few hundred microns and a bias current of a few hundred micro-amperes,  $f_{co}$  closes to 1 MHz [16].

Next,  $n_P(t)$  is divided into a thermal noise component  $n_T(t)$  and a flicker noise component  $n_F(t)$ . Let their power spectra be  $N_T(f)$  and  $N_F(f)$ , the shape of which is shown in Fig. 2.

Previous research [6] has reported that the latch-based method cancels unpreferable components to generate highly random numbers and is capable of mitigating the influence of  $n_F(t)$  and  $n_A(t)$  as much as possible to purify the thermal noise for the TRNG.

### 3 Characteristics of Lowest Significant Bit in Wireless Signal

This section discusses how the noise component behaves after the ADC in single component,  $x(t)$  and  $y(t)$ , particularly at the lowest significant bit (LSB) of the noise component. This discussion can be applied to both components in the same manner because their statistical properties are effectively the same. As a representative of a single component,  $y(t)$  is used in this section.

#### 3.1 Wireless channel noise

The RF signal detected by a receiver comprises not only the transmitted component but also the noise term. Let the detected signal be  $r(t)$ . The transmitted component and noise term are  $u(t)$  and  $n(t)$ , respectively. The noise term  $n(t)$  comprises thermal noise  $n_T(t)$  and other miscellaneous components  $n_O(t)$ , e.g., interference and shot noise. When represented as an equation,  $r(t) = u(t) + n(t) = u(t) + n_T(t) + n_O(t)$ . Note that some interference could be considered white Gaussian when it comes from a large number of interfering stations, for example, in Wi-Fi or cellular systems. Part of other noises generated due to hardware errors may also behave like thermal noise; however, such noises are supposed to be depressed as much as possible for better signal detection in wireless communication. Additive white Gaussian noise (AWGN) is usually assumed in static wireless channels, which follows Gaussian distribution with a flat power spectrum [21].

Flicker noise referred to as  $1/f$  noise, could occur especially in direct conversion receivers which convert the received RF signal to the baseband without intermediate frequency (IF) conversion. In contrast, in SiGe or BiCMOS circuit implementation, which eases  $1/f$  noise, or in wide-band communication systems, whose bandwidths are larger than  $f_{co}$ , the  $1/f$  noise becomes less effective [16]. Low frequency noise is deemed less effective in super-heterodyne receivers, IF and RF sampling receivers referred to as SDRs.

### 3.2 Wireless channel model

In a receiver, the received signal is divided into two components. In the case of coherent detection (Fig. 3),  $r(t)$  is decomposed into in-phase and quadrature-phase components with the reference of a recovered carrier. Likewise, in incoherent detection, there exist two components, which are orthogonal with respect to each other, and a similar model can be applied.

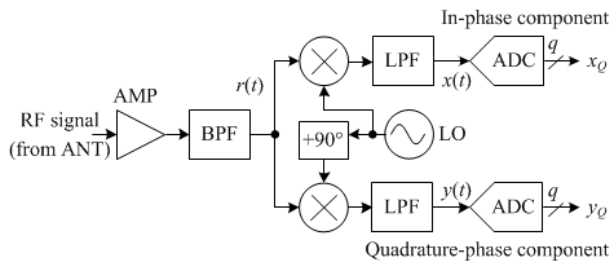


Figure 3: Configuration of coherent demodulator.

Let the carrier frequency be  $f_c$  and the carrier be  $\cos(2\pi f_c t)$ . Then,  $r(t)$  can be expressed as follows:

$$r(t) = x(t) \cos(2\pi f_c t) + y(t) \sin(2\pi f_c t).$$

The first term on the right side of the equation is the in-phase component (I-Ch), and the second term is the quadrature-phase component (Q-Ch). These components contain noise.

In communication theory, the baseband signal can be depicted by the complex number form of  $x(t) + jy(t)$ , which is referred to as the equivalent low-pass signal [21](p.155). In principle, the real components  $x(t)$  and  $y(t)$  are statistically the same. Due to some hardware errors or phase noise in the recovered carrier, IQ imbalance may occur; however, its effect is generally so small that it is considered negligible.

In Fig. 3, both components are quantized as  $x_Q$  and  $y_Q$ , respectively, with  $q$  bits each, and supplied to a digital demodulator to recover the transmitted information.

In the following subsections, we discuss how the noise component behaves after the ADC in  $x(t)$  and  $y(t)$ , particularly at the LSB of noise component.

As mentioned at early part of this section,  $y(t)$  is used as a representative of a single component there.

### 3.3 Quantizing at ADC

The signal  $y(t)$  is sampled at a frequency  $f_s$  and quantized with  $q$  bits, with a quantizing width of  $d$ . Let  $y$  be the sample value, and  $y_Q$  be its quantized symbol. Then, as shown in Fig. 4,  $y_Q = \lfloor y/d \rfloor$ , which is correct as long as  $y(t)$  is in the ADC range. When  $y(t)$  is out of range,  $y_Q$  is clipped, where  $y_Q = 0$  when  $y \leq 0$ , and  $y_Q = (2^q - 1)$  when  $y$  exceeds the limit. Here,  $y(t)$  is assumed to be within the ADC range, which is usually a necessary condition for correctly receiving the wireless signal.

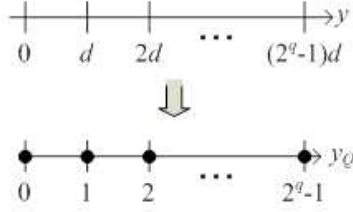


Figure 4: Quantizing.

### 3.4 Ideal distribution

Let the LSB of  $y_Q$  be  $Y$ , then  $Y$  can be expressed as follows:

$$Y = (y \bmod 2d) \stackrel{\leq}{\geq} d$$

where  $x \stackrel{\leq}{\geq} d$  is 0 when  $x \leq d$ , and 1 when  $x > d$ .

By dividing the analog sample value  $y$  into the noise term  $n$  required for TRNG and the other term  $s$ ,  $y$  can be expressed as  $y = s + n$ . Here,  $n$  is an unpredictable component containing thermal noise at least, which follows Gaussian distribution. Other unpreferred component for TRNG is  $s$ , which comprises at least a modulated signal from the desired transmitter for communication purpose.

When the analog modulus signal  $\tilde{y} = y \bmod 2d$  is defined, it can also be expressed as follows:

$$\begin{aligned} \tilde{y} &= y \bmod 2d = (s + n) \bmod 2d \\ &= [(s \bmod 2d) + (n \bmod 2d)] \bmod 2d \\ &\equiv (\tilde{s} + \tilde{n}) \bmod 2d. \end{aligned} \tag{1}$$

With a sufficiently small  $d$  value, the modulus noise term  $\tilde{n}$  is uniformly distributed in  $[0, 2d)$  [22]. Then, as shown in Fig. 5, it is understood that  $\tilde{y}$  also

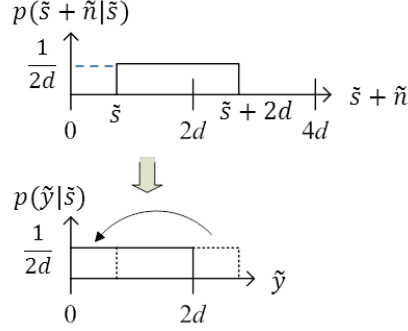


Figure 5: The pdf of  $\tilde{y}$ .

follows a uniform distribution regardless of  $\tilde{s}$ . Therefore, the following equation holds with respect to the following probability density function (PDF)  $p(\cdot)$ :

$$p(\tilde{y}) = \int p(\tilde{y}|\tilde{s})p(\tilde{s})d\tilde{s} = \frac{1}{2d} \int p(\tilde{s})d\tilde{s} = \frac{1}{2d}.$$

Consequently, since  $Y = \tilde{y} \stackrel{\leq}{\geq} d$ , it is understood that  $p(Y) = 1/2$ .

### 3.5 Realistic distribution

Assuming that  $d$  is not necessarily small and  $n$  follows zero-mean Gaussian distribution with a standard deviation  $\sigma$ , this subsection clarifies the deviation for the probability of  $Y \in \{0, 1\}$  from  $1/2$ . At first, the PDF of  $\tilde{n}$  with the quantization width  $d$ ,  $p_{\tilde{n}}(\tilde{n}, 2d)$ , is formulated as follows<sup>1</sup>:

$$\begin{aligned} p_{\tilde{n}}(\tilde{n}, 2d) &= \sum_{l=-\infty}^{\infty} p_n(n - 2ld) \\ &= \frac{1}{\sqrt{2\pi}\sigma} \sum_{l=-\infty}^{\infty} e^{-\frac{(\tilde{n}-2ld)^2}{2\sigma^2}}. \end{aligned} \quad (2)$$

Its outline is shown in Fig. 6 as  $2d = 3.0$ .

The conditional probability of sign  $Y$ , i.e.,  $p(Y|\tilde{s})$ , is expressed as follows:

$$p(Y = 0|\tilde{s}) = \int_0^d p(\tilde{y}|\tilde{s})d\tilde{y} = 1 - p(Y = 1|\tilde{s}), \quad (3)$$

$$p(\tilde{y}|\tilde{s}) = \frac{1}{\sqrt{2\pi}\sigma} \sum_{l=-\infty}^{\infty} e^{-\frac{(\tilde{y}-\tilde{s}-2ld)^2}{2\sigma^2}}. \quad (4)$$

<sup>1</sup>It can be expressed with the theta function [22].

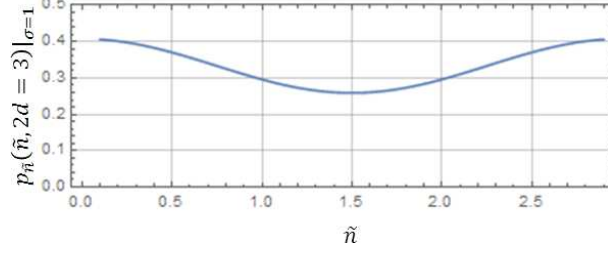


Figure 6: Overview of  $p_{\tilde{n}}(\tilde{n}, 2d = 3)$  at  $\sigma = 1$ .

Let the deviation from equal probability  $1/2$  be  $\Delta(\tilde{s}, 2d)$  as follows:

$$p(Y = 0|\tilde{s}) = \frac{1}{2} + \Delta(\tilde{s}, 2d), \quad (5)$$

$$p(Y = 1|\tilde{s}) = \frac{1}{2} - \Delta(\tilde{s}, 2d). \quad (6)$$

Therefore,

$$\Delta(\tilde{s}, 2d) = \int_0^d p(\tilde{y}|\tilde{s})d\tilde{y} - \frac{1}{2}.$$

The outline of  $\Delta(\tilde{s}, 2d = 3)$  as  $2d = 3$  is shown in Fig. 7, and the deviation of  $\Delta(\tilde{s}, 2d = 3)$  is dependent on  $s$ .

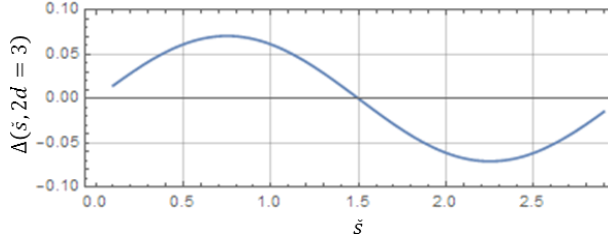


Figure 7: Overview of  $\Delta(\tilde{s}, 2d = 3)$  at  $\sigma = 1$ .

Considering that the other term  $s$  represents a transmission signal or  $1/f$  noise,  $s$  seems time-invariant in the sampling period  $1/f_s$ . Therefore, we evaluate the deviation as its worst (largest) value, which appears when  $\tilde{s} = d \pm d/2$ . Then, the largest deviation  $\Delta'(d/\sigma)$  can be expressed as follows:

$$\begin{aligned} \Delta' \left( \frac{d}{\sigma} \right) &= \Delta \left( \tilde{s} = \frac{d}{2}, 2d \right) = \int_0^d p \left( \tilde{y} | \tilde{s} = \frac{d}{2} \right) d\tilde{y} - \frac{1}{2} \\ &= \frac{1}{\sqrt{2\pi}\sigma} \sum_{l=-\infty}^{\infty} \int_0^{\frac{d}{\sigma}} e^{-\frac{(\tilde{y} - \frac{d}{2\sigma} - \frac{2ld}{\sigma})^2}{\sigma}} d\tilde{y}. \end{aligned} \quad (7)$$

The outline depicted in Fig. 8 shows, for example, the deviation is less than 0.01 when the quantizing width  $d$  is equal to the standard deviation of thermal noise,  $\sigma$ . When  $d/\sigma$  is less than  $3/4$ , the deviation is around  $10^{-4}$  or less.

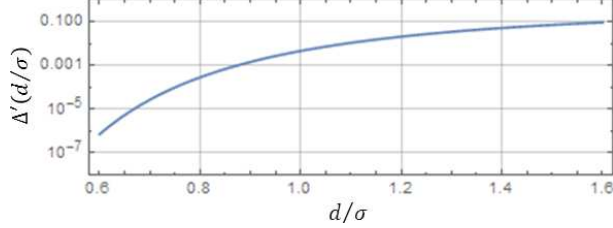


Figure 8: Overview of  $\Delta'(\frac{d}{\sigma})$ .

From the viewpoint of communication theory, since  $\tilde{s}$  is considered as quantizing noise, its distribution is considered uniform, i.e.,  $p(\tilde{s}) = 1/(2d)$ . Therefore, on long-time average, the total deviation is expected to be 0 so that  $Y$  becomes 0 or 1 in equal probability.

$$\begin{aligned} p(Y = 0) &= \frac{1}{2d} \int_0^{2d} p(Y = 0|\tilde{s}) d\tilde{s} \\ &= \frac{1}{2} + \int_0^{2d} \Delta(\tilde{s}, 2d) d\tilde{s} = \frac{1}{2} \end{aligned}$$

### 3.6 Entropy

In contrast to the well-known Shannon entropy, which is considered to be average unpredictability, minimum entropy is the smallest unpredictability of outcomes, which is described as follows:

$$\begin{aligned} \min H\left(\frac{d}{\sigma}\right) &= -\log_2 \max\left(\frac{1}{2} + \Delta(\tilde{s}, 2d)\right) \\ &= -\log_2\left(\frac{1}{2} + \Delta'\left(\frac{d}{\sigma}\right)\right) \\ &\simeq 1 - 2.885 \Delta'\left(\frac{d}{\sigma}\right). \end{aligned} \tag{8}$$

This is shown in Fig. 9. It is more than around 0.8 bit when  $d/\sigma \leq 1.5$ .

### 3.7 Neighbor bit correlation

To explain neighbor correlation, here the sample number is introduced with subscript notation. For example, the  $i$ -th sample of  $y$  is written as  $y_i$ . Then

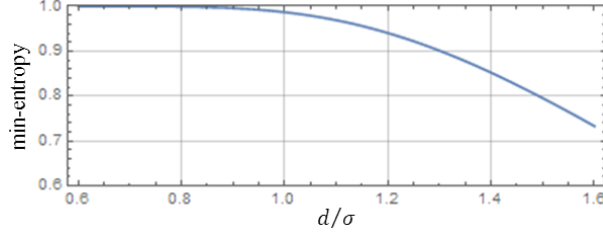


Figure 9: Theoretical min-entropy for single channel.

neighboring symbol correlation  $\rho$  of  $y$  is expressed as follows:

$$\begin{aligned}\rho &= \frac{E[y_i y_{i+1}] - \bar{y}^2}{\text{Var}[y]} = \frac{E[(s_i + n_i)(s_{i+1} + n_{i+1})]}{E[(s + n)^2]} \\ &= \frac{\bar{s}^2}{\bar{s}^2 + \bar{n}^2}.\end{aligned}\quad (9)$$

In Eqn. (9), it is assumed that  $s$  and  $n$  are not correlated each other and are 0 on average. Moreover their neighbor symbol correlations are 1 for  $s$  and 0 for  $n$ . This equation indicates that there is a general autocorrelation in the input signal to the receiver.

Next we consider a neighbor bit correlation of the generated random number sequence. Because  $Y$  is 0 or 1, the average  $\bar{Y}$  is equal to the squared average  $\bar{Y}^2$ .

$$\begin{aligned}\bar{Y} &= p(Y = 1) = \bar{Y}^2 \\ &= \int_0^{2d} p(Y = 1|\tilde{s})p_{\tilde{s}}(\tilde{s})d\tilde{s} \\ &= \int_0^{2d} \Delta(\tilde{s}, 2d)p_{\tilde{s}}(\tilde{s})d\tilde{s} - \frac{1}{2} \\ &\equiv \bar{\Delta}\left(\frac{d}{\sigma}\right) - \frac{1}{2}\end{aligned}\quad (10)$$

$$(11)$$

The deviation of  $Y$  is expressed as follows:

$$\text{Var}[Y] = \bar{Y}^2 - (\bar{Y})^2 = \frac{1}{4} - \bar{\Delta}^2\left(\frac{d}{\sigma}\right).\quad (12)$$

Expectation of the product between neighbor bits is expressed as

$$\begin{aligned}E[Y_i Y_{i+1}] &= \int_0^{2d} \int_0^{2d} p(Y_i = 1|\tilde{s}_i)p(Y_{i+1} = 1|\tilde{s}_{i+1}) \\ &\quad p_{\tilde{s}}(\tilde{s}_i, \tilde{s}_{i+1})d\tilde{s}_i d\tilde{s}_{i+1}.\end{aligned}$$

Since the correlation between neighboring symbols  $s$  is 1, following formula holds:

$$p_{\tilde{s}}(\tilde{s}_i, \tilde{s}_{i+1}) = \delta_D(\tilde{s}_{i+1} - \tilde{s}_i)p_{\tilde{s}}(\tilde{s}_i),$$

where  $\delta_D$  is Dirac's delta function. Next,

$$\begin{aligned} E[Y_i Y_{i+1}] &= \int_0^{2d} p(Y_i = 1 | \tilde{s}_i)^2 p_{\tilde{s}}(\tilde{s}_i) d\tilde{s}_i \\ &= \int_0^{2d} \left( \frac{1}{2} - \Delta(\tilde{s}, 2d) \right)^2 p_{\tilde{s}}(\tilde{s}_i) d\tilde{s}_i \\ &= \frac{1}{4} - \bar{\Delta} \left( \frac{d}{\sigma} \right) + \int_0^{2d} \Delta(\tilde{s}, 2d)^2 p_{\tilde{s}}(\tilde{s}_i) d\tilde{s}_i \\ &\equiv \frac{1}{4} - \bar{\Delta} \left( \frac{d}{\sigma} \right) + \bar{\Delta}^2 \left( \frac{d}{\sigma} \right). \end{aligned} \quad (13)$$

Therefore, the neighbor bit correlation  $R$  is as follows:

$$\begin{aligned} R &= \frac{E[Y_i Y_{i+1}] - (\bar{Y})^2}{\text{Var}[Y]} = \frac{\bar{\Delta}^2 - (\bar{\Delta})^2}{1/4 - (\bar{\Delta})^2} \\ &\simeq 4\bar{\Delta}^2 - (\bar{\Delta})^2. \end{aligned} \quad (14)$$

These equations indicate the existence of a neighbor bit correlation in the sign  $Y$  sequence if  $\tilde{s}$  varies slowly and  $p(Y)$  is not a perfect 1/2.

The maximum of  $|R|$  is then estimated, which is given by the distribution of  $\tilde{s}$ ,  $p_{\tilde{s}}(\tilde{s})$ , such that

$$p_{\tilde{s}}(\tilde{s}) = \frac{1}{2} \left( \delta_D \left( \tilde{s} - \frac{d}{2} \right) + \delta_D \left( \tilde{s} - \frac{3d}{2} \right) \right). \quad (15)$$

Then  $\bar{\Delta} = 0$  and  $\bar{\Delta}^2 = \Delta^2(\tilde{s} = d/2, 2d) = 4\Delta'^2(d/\sigma)$ ; therefore,

$$R \simeq 4 \Delta'^2 \left( \frac{d}{\sigma} \right). \quad (16)$$

From the graph shown in Fig. 10, maximum  $|R|$  is less than  $10^{-4}$  as  $d/\sigma \leq 1.0$ .

### 3.8 Out of range case at ADC

As discussed previously, the input analog signal is assumed to be within the ADC input range. If it is out of the range, the maximum or minimum values are output as a quantized signal. When this occurs to a substantial degree, the characteristics of the LSB can become unpreferable with respect to randomness. In this case, the signals cannot be correctly received at the terminal. Then, in general, wireless systems are supposed to prevent the terminal from initiating the communication because it does not receive the system information necessary

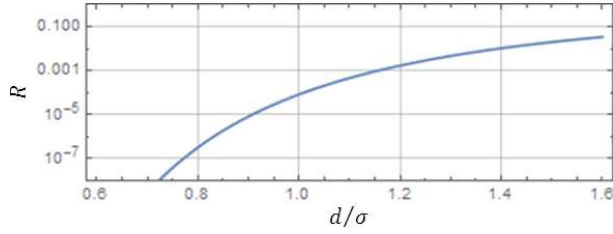


Figure 10: Adjacent bit correlation for a single channel.

for sending the signal. If the signal is not received correctly when the terminal has already begun the communication, the terminal would transmit a negative acknowledge message or retransmit the same message that was sent previously. Each case does not require a new random number because the terminal cannot transmit a new message. This feature in wireless communication systems alleviates the out-of-ADC-range issue in the proposed TRNG scheme.

## 4 Proposed TRNG Scheme

### 4.1 System concept

Figure 11 shows the functional location of the proposed TRNG in a wireless system, wherein DUP/SW is a duplexer or switch utilizing a single antenna for both transmission and reception, with RX being the receiving circuit, TX serving as the transmission circuit, and proc. representing the information processor. As mentioned previously, a wireless terminal is required to receive the signal from the base station prior to its transmission in general wireless systems because it should get system information and/or permission to transmit from the network side. It is sufficient for the TRNG to work during the reception process at the terminal.

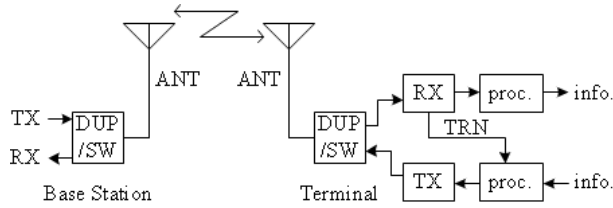


Figure 11: System concept.

## 4.2 Configuration

The proposed scheme utilizes a part of the communication circuit for the TRNG in which  $d/\sigma$  might not be small depending on the input signal level. To cope with this situation, the proposed scheme uses an XOR operation between  $X$  and  $Y$  (i.e.,  $Z = X \oplus Y$ ) as shown in Fig. 12. It is known that the XORed sequence

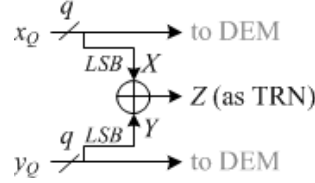


Figure 12: Configuration for TRNG.

between independent binary sequences has better randomness [9] especially on a balance of logical 0 and 1. Due to the principle of independency between I and Q components,  $X$  and  $Y$  are also independent each other, therefore  $Z$  is expected to have better frequency on 0 and 1. Even with the clipping case when the input level is high, the balance of 0 and 1 at the sequence on  $Z$  will not collapse so much because simultaneous saturation on both the I and Q components rarely occurs.

## 4.3 Random number average

As mentioned previously, the I and Q components are ideally supposed to be independent. However, from a practical standpoint, it is worthwhile to study the effect of the correlation between both components on random number  $Z$ , because the independency may not be perfect due to certain hardware errors.

Let the joint probability  $p(X, Y)$  be defined as equations in Table 1. In

Table 1: Joint probability with correlation parameter,  $r$

	$Y = 0$	$Y = 1$	$p(X)$
$X = 0$	$(\frac{1}{2} + \Delta_1)(\frac{1}{2} + \Delta_2) + r$	$(\frac{1}{2} + \Delta_1)(\frac{1}{2} - \Delta_2) - r$	$\frac{1}{2} + \Delta_1$
$X = 1$	$(\frac{1}{2} - \Delta_1)(\frac{1}{2} + \Delta_2) - r$	$(\frac{1}{2} - \Delta_1)(\frac{1}{2} - \Delta_2) + r$	$\frac{1}{2} - \Delta_1$
$p(Y)$	$\frac{1}{2} + \Delta_2$	$\frac{1}{2} - \Delta_2$	

Table 1,  $\Delta_i = \Delta(\tilde{s}_i, 2d)$ ,  $\tilde{s}_1$  and  $\tilde{s}_2$  are other modulus components in I-Ch and Q-Ch, respectively. The term  $r$  determines the correlation between  $X$  and  $Y$ . When  $r = 0$ , there is no correlation between  $X$  and  $Y$ .

Then, the following equations hold:

$$\begin{aligned}
E[XY] - \bar{X}\bar{Y} &= \left(\frac{1}{2} - \tilde{s}_1\right) \left(\frac{1}{2} - \tilde{s}_2\right) + r \\
&\quad - \left(\frac{1}{2} - \tilde{s}_1\right) \left(\frac{1}{2} - \tilde{s}_2\right) \\
&= r \\
\text{Var}[X] &= \frac{1}{2} - \Delta_1 - \left(\frac{1}{2} - \Delta_1\right)^2 = \frac{1}{4} - \Delta_1^2 \\
\text{Var}[Y] &= \frac{1}{2} - \Delta_2 - \left(\frac{1}{2} - \Delta_2\right)^2 = \frac{1}{4} - \Delta_2^2
\end{aligned}$$

Therefore, the correlation between  $X$  and  $Y$  is nearly  $4r$ .

$$\frac{E[XY]}{\sqrt{\text{Var}[X]\text{Var}[Y]}} \simeq 4r \tag{17}$$

The probability of  $Z$  can be expressed as follows:

$$\begin{aligned}
p(Z = 0|\tilde{s}_1, \tilde{s}_2) &= \left(\frac{1}{2} + \Delta_1\right) \left(\frac{1}{2} + \Delta_2\right) + r \\
&\quad + \left(\frac{1}{2} - \Delta_1\right) \left(\frac{1}{2} - \Delta_2\right) + r \\
&= \frac{1}{2} + 2\Delta(\tilde{s}_1, 2d)\Delta(\tilde{s}_2, 2d) + 2r \\
p(Z = 1|\tilde{s}_1, \tilde{s}_2) &= \frac{1}{2} - 2\Delta(\tilde{s}_1, 2d)\Delta(\tilde{s}_2, 2d) - 2r.
\end{aligned}$$

Therefore, the maximum deviation of  $Z$  is improved, compared with that of  $Y$  given by Eqn. (7), as follows:

$$2\Delta'^2 \left(\frac{d}{\sigma}\right) + 2r.$$

Figure 13 plots the maximum deviation of  $Z$  for  $r = 0$  with the dashed line, and for  $r = 10^{-4}$  with the solid line. For both cases, the maximum deviation of  $Z$  becomes less than 0.01 as  $d/\sigma \leq 1.5$ .

#### 4.4 Entropy evaluation

The estimated minimum entropy is as follows:

$$\begin{aligned}
\min H\left(\frac{d}{\sigma}\right) &= -\log_2 \max p(Z|\tilde{s}_1, \tilde{s}_2) \\
&= -\log_2 \left(\frac{1}{2} + 2\Delta'^2 \left(\frac{d}{\sigma}\right) + 2r\right) \\
&\simeq 1 - 5.771 \left(\Delta'^2 \left(\frac{d}{\sigma}\right) + r\right). \tag{18}
\end{aligned}$$

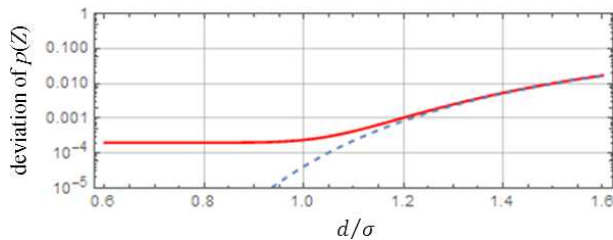


Figure 13: Deviation of  $p(Z)$  for proposed TRNG. (dashed line for  $r = 0$ , solid line for  $r = 10^{-4}$ )

This is shown in Fig. 14 wherein the dashed line represents the case of  $r = 0$ , while the solid line depicts the case of  $r = 10^{-4}$ . The lines show nearly identical curves. In both cases, the minimum entropy is around 0.95 bit as  $d/\sigma \leq 1.5$ .

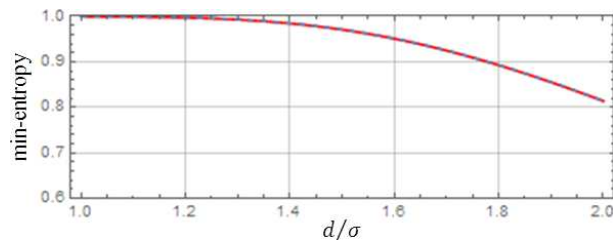


Figure 14: Theoretical minimum entropy for proposed TRNG. (dashed line for  $r = 0$ , solid line for  $r = 10^{-4}$ )

## 5 Experimental Verification

### 5.1 Experimental system

With a multipurpose receiver, the feasibility of the proposed scheme is verified in this section. This receiver outputs the sequences of  $x_Q$  and  $y_Q$  in Fig. 3 to a PC. The experimental system in Fig. 15 comprises a signal generator outputting a simulated version of the desired signal for communication, two closely located antennas for transmission and reception in a shield box, and a multipurpose receiver. The primary conditions are summarized in Table 2.

The receiver adopts a super-heterodyne configuration wherein the signal is sampled at an IF band having a center frequency of 3.57 MHz, which is then converts to I and Q baseband components using digital processing.

As a desired signal, the PN9 sequence is used with QPSK modulation whose symbol rate is 128 kbps. Its center frequency is assumed to be the 920 MHz band which is used for telemeters, telecontrols, and data transmission facilities in Japan [26] The sampling frequency is 256 Ksample/s, assuming that there

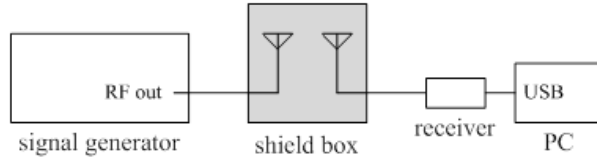


Figure 15: Experimental system.

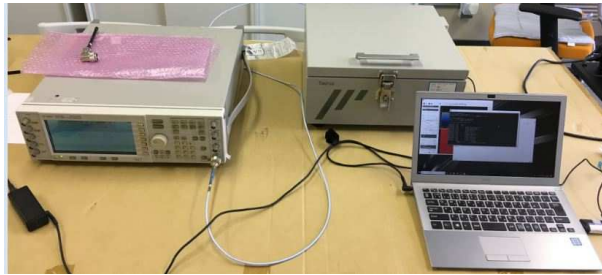


Figure 16: Experimental equipments.

Table 2: Test conditions

Transmitter	
Signal generator	Agilent E4432B [23]
Center frequency	923.6 MHz
Baseband signal	PN9
Bandpass filter	Root Nyquist with 0.5 roll-off
Modulation	QPSK
Symbol rate	128 ksps
Receiver	
Device	R820T [27]
Sampling frequency	256 kHz
Number of quantizing bits	8 for each channel
Environment	
Temperature	19°C
Measurement duration	20 s.
# of TRN	5,120,000 bits

are two over-samples. Note that using `rtl_test` command [25], it was confirmed that the measurement data had not been dropped at the PC.

At the receiver R820T working AGC, output characteristics have been observed as a function of input level. The purpose is to verify the deviation of the random number  $Z$ , which is dependent on the circuit gain.

## 5.2 Full bit characteristics

To confirm the gain characteristics of the experimental configuration, the relationship between the output level  $P_{out}$  of the transmitter and the average square of quantized symbols was determined. For reference, a case of no desired signal, i.e.,  $P_{out} = -\infty$ , is also measured. The amplifying gain is an important parameter for a TRNG, so as to gather the noise component. The receiver automatically controls the gain to adequately amplify the input signal within the ADC range. When the input signal level is high, the gain becomes low. Subsequently, the noise might be depressed and  $d/\sigma$  becomes high, therefore, the randomness of the generated random numbers might be worse. In case that the input signal level is considerably high, the terminal cannot receive any signal correctly, so it is usually not permitted to transmit new messages. In such case, the TRNG is not necessary to work.

Figure 17 plots the deviation of quantized sample values,  $\overline{|x_Q|^2 + |y_Q|^2}$ , when the RF output varies. Because of 8-bit ADC for each channel, its maximum value is  $2^{7 \times 2} = 16384$ . According to this figure, the quantized signal becomes saturated as  $P_{out} \geq -20$  dBm. Therefore, the case of  $P_{out} < -20$  dBm is crucial in which the following examinations should be passed.

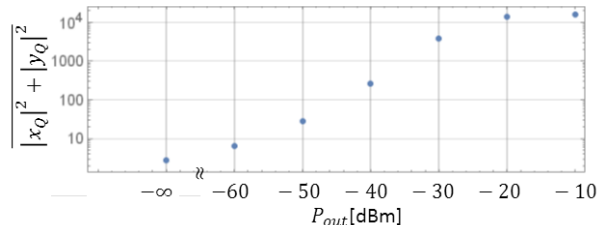


Figure 17: Average squared signal property.

## 5.3 Minimum entropy evaluation

Based on NIST 800-90B [29], we also evaluate the generated random number sequence. As previously discussed, the sequence is ideally assumed to be independent and identically distributed (IID), with adequate gain control and negligible errors. Thus, it should be verified with the IID assumption test. We also estimate the minimum entropy with non-IID assumption through various methods [29].

Table 3: Results for iid test and non-iid min-entropy estimation

$P_{out}$ [dBm]	$-\infty$	-60	-50	-40	-30	-20	-10
IID Assumption Test	Passed	Passed	Passed	Passed	Passed	Failure	Failure
Most Common Value	0.997677	0.998092	0.997974	0.998436	0.998126	0.997791	0.998285
Collision	0.961081	0.944718	0.955606	0.939304	0.944718	0.771181	0.716912
Markov	0.998736	0.998976	0.998808	0.997549	0.998341	0.958014	0.935486
Compression	1.000000	1.000000	1.000000	0.963826	0.988773	0.814660	0.773437
t-Tuple	0.936624	0.941863	0.938330	0.933322	0.936624	0.907921	0.862752
LRS	0.986174	0.998485	0.961189	0.994343	0.927136	0.961189	0.982639
Multi MCW	0.998724	0.998746	0.998506	0.998564	0.998492	0.998626	0.999607
Lag	0.999024	0.999202	0.998301	0.998575	0.998308	0.958166	0.934990
Multi MMC	0.997938	0.999121	0.998551	0.998142	0.998242	0.944350	0.904267
LZ78Y	0.997748	0.998269	0.998955	0.997668	0.998369	0.958158	0.934980
Min-entropy	0.936624	0.941863	0.938330	0.933322	0.927136	0.771181	0.716912

The IID assumption test comprises 11 permutation tests and 3 chi-square statistical tests. The evaluation results show that the IID assumption is rejected with type I error probability of 0.001 in a permutation test when  $P_{out} \geq -20$  dBm. Similarly, for  $P_{out} < -20$  dBm, the estimated minimum entropy is at around 0.93, but for  $P_{out} \geq -20$  dBm, it declines to around 0.7. According to Table 7 of a previous study [9], the minimum entropies of conventional methods are estimated to be in the range 0.47 to 0.93. Based on this, our results are considered satisfactory.

#### 5.4 NIST statistical test

The NIST statistical test comprises 15 test items for evaluating randomness of random sequence [30]. Parameters of block length defined in the test are set as shown in Table 4 so that all values are in recommended ranges. The measured sequence was divided into five streams. Each stream was 1,024,000 bits long and the statistical test was performed every stream. For 12 specific examination tests whose results are not too long to be displayed, the results are summarized in Table 5. The pass rate 4/5 means that the test has finally passed through 5 streams when 4 or more streams have passed the test item.

As for Table 5, the successful ratio is 5/5, except for 2 points, one of which is a ‘‘Cumulative Sums’’ test at  $P_{out} = -40$ , while the other is an ‘‘FFT’’ test at  $P_{out} = -\infty$  dBm. Among all 15 tests, only the case of  $P_{out} = -10$  dBm exhibits failure. The failed test occurred at one of the 148 templates in a ‘‘non overlapping template test,’’ wherein only 3 streams have passed among 5 streams. As a result, the test fails at  $P_{out} = -10$  dBm and passes at  $P_{out} \leq -20$  dBm.

Table 4: Block length for statistical tests

Block Frequency, $M$	128
Non-Overlapping Template, $m$	9
Overlapping Template, $m$	9
Approximate Entropy, $m$	10
Serial, $m$	16
Linear Complexity, $M$	500

Table 5: 12 of 15 tests and total results for 5 streams (pass rate 4/5)

$P_{out}$ [dBm]	$-\infty$	-60	-50	-40	-30	-20	-10
Frequency	5/5	5/5	5/5	5/5	5/5	5/5	5/5
Block Frequency	5/5	5/5	5/5	5/5	5/5	5/5	5/5
Cum. Sums (F)	5/5	5/5	5/5	5/5	5/5	5/5	5/5
Cum. Sums (R)	5/5	5/5	5/5	4/5	5/5	5/5	5/5
Runs	5/5	5/5	5/5	5/5	5/5	5/5	5/5
Longest Run	5/5	5/5	5/5	5/5	5/5	5/5	5/5
Rank	5/5	5/5	5/5	5/5	5/5	5/5	5/5
FFT	4/5	5/5	5/5	5/5	5/5	5/5	5/5
Overlap.Template	5/5	5/5	5/5	5/5	5/5	5/5	5/5
Universal	5/5	5/5	5/5	5/5	5/5	5/5	5/5
Approx. Entropy	5/5	5/5	5/5	5/5	5/5	5/5	5/5
Serial (F)	5/5	5/5	5/5	5/5	5/5	5/5	5/5
Serial (R)	5/5	5/5	5/5	5/5	5/5	5/5	5/5
Linear Complex.	5/5	5/5	5/5	5/5	5/5	5/5	5/5
Total results	Pass	Pass	Pass	Pass	Pass	Pass	Fail

## 6 Conclusion

The conventional TRNG using the MSB of the noise level should exclude predictable components as much as possible. In contrast, this paper proposes a TRNG method based on the LSB of the noise level for terminals in wireless systems. We discussed the method with a theoretical AWGN model and evaluated its minimum entropy with several statistical tests from a practical perspective with a general receiver.

The proposed method is suitable for embedding in wireless terminals due to few additional circuits and processing. Not only user terminals but also wireless sensors or small IoT terminals for machine-to-machine communications are examples of preferable applications of the proposed method. The results of NIST statistical tests and min-entropy estimation displayed reasonably good performance unless the received signal exceeded the saturation level. When the input signal level is considerably high (which may occur intentionally), the signal will be distorted at the receiver and cannot be demodulated. In this case, as a general operation in wireless communication systems, the terminal will not transmit renewed information (i.e., the terminal does not need a random number under the degraded conditions of the proposed TRNG scheme). These results show that the proposed TRNG scheme is reasonably effective and efficient.

## Acknowledgments

This work was supported by the Japan Society for the Promotion of Science KAKENHI Grant Number 25330157.

## References

- [1] N. Heninger, Z. Durumeric, E. Wustrow, J. A. Halderman, “Mining Your Ps and Qs: Detection of Widespread Weak Keys in Network Devices,” In Proc. 21st USENIX Security Symposium, Aug. 2012, Rev.2 July 11 2012.
- [2] M. Bellare, S. Goldwasser and Micciancio, “Pseudo-random number generation within cryptographic algorithms: the DSS case,” In Proc. of Crypto 97, LNCS 1294. IACR, Palo Alto, CA. Springer-Verlag, Berlin 1997.
- [3] C. S. Petrie, and A. Connelly, “A Noise-Based IC Random Number Generator for Applications in Cryptography,” IEEE Trans. on Circuits and Systems I: Fundamental Theory and Applications, vol. 47, no. 5, pp. 615-621, 2000.
- [4] W. T. Holman, J. A. Connelly, and A. Dowlatabadi, “An integrated analog/digital random noise source,” IEEE Trans. Circuits Syst. I, vol. 44, June 1997.
- [5] W. Chen, W. Che, Z. Bi, J. Wang, N. Yan, X. Tan, J. Wang, H. Min, and J. Tan, “A 1.04 $\mu$ W truly random number generator for Gen2 RFID tag,” in

- Solid-State Circuits Conference, 2009. A-SSCC 2009. IEEE Asian, Nov. 2009, pp. 117-120.
- [6] J. Holleman, S. Bridges, B. P. Otis, and C. Diorio, "A  $3\mu\text{W}$  CMOS True Random Number Generator With Adaptive Floating-Gate Offset Cancellation," *IEEE Journal of Solid-State Circuits*, vol. 43, no. 5, pp. 1324-1336, 2008.
- [7] H. Zhun and C. Hongyi, "A truly random number generator based on thermal noise," In proceedings of the International Conference on ASIC, pp. 862-864, 2001.
- [8] G. K. Balachandran and R. E. Barnett, "A 440-nA True Random Number Generator for Passive RFID Tags," *IEEE Trans. on Circuits and Systems I: Fundamental Theory and Applications*, vol. 55, no. 11, pp. 3723-3732, 2008.
- [9] K. Lee, S. Lee, C. Seo, and K. Yim, "TRNG (True Random Number Generator) method using visible spectrum for secure communication on 5G network", DOI 10.1109, *IEEE Access*, pp. 12838-12847(2018).
- [10] J. Voris, N. Saxena, and T. Halevi, "Accelerometers and randomness: perfect together," *Security - WISEC 2011*. Hamburg, Germany: ACM, pp.115-126, June 2011.
- [11] K. Wallace, K. Moran, Ed Novak, G. Zhou and Kun Sun, "Toward Sensor-Based Random Number Generation for Mobile and IoT Devices," *IEEE Internet of Things Journal*, vol. 3, no. 6, pp. 1189-1201, Dec. 2016.
- [12] A. Francillon and C. Castelluccia, "TinyRNG: A Cryptographic Random Number Generator for Wireless Sensor Network Nodes," in *Symposium on Modeling and Optimization in Mobile, Ad Hoc, and Wireless Networks, IEEE WiOpt 2007*. Limassol, Cyprus: IEEE, April 2007.
- [13] R. Latif and M. Hussain, "Hardware-based random number generation in Wireless Sensor Networks (WSNs)," *Advances in Information Security and Assurance*, pp. 732740, 2009.
- [14] C. Hennebert, H. Hicham, and L. Cedric, "The entropy of wireless statistics," *Proceedings of the 2014 European Conference on Networks and Communications (EuCNC)*, pp. 1-5, 2014.
- [15] F. A. Levinzon and L. K. J. Vandamme, "Comparison of  $1/f$  noise in JFETs and MOSFETs with several figures of merit," *Fluctuation and Noise Letters*, Vol. 10, no. 4, pp.447-465, 2011.
- [16] Q. Gu, *RF System Design of Transceivers for Wireless Communications*, pp.154-155, Springer, 2005.
- [17] [http://www.fdk.com/cyber-e/pi Lic\\_rpg100.html](http://www.fdk.com/cyber-e/pi Lic_rpg100.html)

- [18] <http://www.silego.com/products/668/312/True-Random-Number-Generator-Hardware.html>
- [19] K. Yamaguchi, and K. Nakamura, "HW-based Random Bit Sequence Generation Method Using Gettime Function," Proceedings of the International Symposium on Information Theory and its Applications (ISITA), Auckland, New Zealand, Dec. 7-10, 2008.
- [20] C. Hennebert, H. Hossayni, and C. Lauradoux, "The Entropy of Wireless Statistics," Proceedings of the 2014 European Conference on Networks and Communications (EuCNC), pp. 1-5, 2014.
- [21] J. G. Proakis, *Digital Communications - Third Ed.*, McGraw-Hill, 1995.
- [22] N. I. Koblitz, *Introduction to Elliptic Curves and Modular Forms - 2nd Ed.*, eq.(4.11) in p.73, Springer, 1993.
- [23] <http://literature.cdn.keysight.com/litweb/pdf/5966-1010J.pdf>
- [24] C. Laufer, *The Hobbyist's Guide to the RTL-SDR: Really Cheap Software Defined Radio - Third Ed.*, Createspace Independent Pub, 2015.
- [25] <https://osmocom.org/projects/sdr/wiki/rtl-sdr>
- [26] <https://www.arib.or.jp/english/html/overview/doc/5-STD-T108v1.0-E1.pdf>
- [27] <https://www.rtl-sdr.com/buy-rtl-sdr-dvb-t-dongles/>
- [28] R. W. Stewart, K. W. Barlee, D. S. W. Atkinson, *Software Defined Radio Using MATLAB & Simulink and the Rtl-Sdr*, pp.10-19, Strathclyde Academic Media, 2015.
- [29] NIST, Recommendation for the Entropy Sources Used for Random Bit Generation, [https://csrc.nist.gov/csrc/media/publications/sp/800-90b/draft/documents/sp800-90b\\_second\\_draft.pdf](https://csrc.nist.gov/csrc/media/publications/sp/800-90b/draft/documents/sp800-90b_second_draft.pdf)
- [30] NIST, A Statistical Test Suite for Random and Pseudo-random Number Generators for Cryptographic Applications, <http://nvlpubs.nist.gov/nistpubs/Legacy/SP/nistspecialpublication800-22r1a.pdf>